CTLs are obtained from the same ethnic group. In addition, by adopting other immunophenotyping readouts such as production of IL-2 from $CD4^+$ T cells, this method could be applied to identification of MHC class II–restricted minor H antigens which have crucial roles in controlling CTL functions upstream. This may open a new field in the study of allo-HSCT since MHC class II–restricted mHags have been technically difficult to identify by conventional methods.

Finally, the discovery of ACC-1^C as a novel minor H antigen indicates that all the mismatched transplants at this locus could be eligible for allo-immune therapies, since we have previously demonstrated that the counter allele also encodes a minor H antigen, ACC-1^Y, which is preferentially expressed and presented on blood components including leukemic cells and may serve as a target of allo-immunity.[7,34] Indeed, CTLs specific for ACC-2, an HLA-B44–restricted minor H antigen restricted by the third exonic SNP on *BCL2A1*,[7] was independently isolated from the peripheral blood of a patient with recurrent leukemia re-entering complete remission after donor lymphocyte infusion.[32] The number of eligible allo-HSCT recipients has now been effectively doubled, accounting for 50% of transplants with HLA-A24 or 20% of all transplantations performed in the Asian population. In conclusion, we have described a simple but powerful method for minor H mapping to efficiently accelerate the discovery of novel minor H antigens that will be needed to contribute to our understanding of the molecular mechanism of human allo-immunity.

Acknowledgments

The authors thank Dr W. Ho for critically reading the manuscript; Dr Keitaro Matsuo, Dr Hiroo Saji, Dr Etsuko Maruya, Dr Mamoru Ito, Ms Keiko Nishida, Dr Ayako Demachi-Okamura, Ms Yasuko Ogino, Ms Hiromi Tamaki, and the staff members of the transplant center, donor centers, and the Japan Marrow Donor Program office for their generous cooperation and expert technical assistance.

This study was supported in part by Scientific Research on Priority Areas (B01; no.17016089) from the Ministry of Education, Culture, Science, Sports, and Technology, Japan; Research on Human Genome, Tissue Engineering Food Biotechnology and the Second and Third Team Comprehensive 10-year Strategy for Cancer Control (no. 26), from the Ministry of Health, Labor, and Welfare, Japan; and a Grant-in-Aid from Core Research for Evolutional Science and Technology (CREST) of Japan.

Authorship

Contribution: T.K. performed most immunologic experiments and preparation of pooled DNA and quantative PCR, analyzed data, and wrote the manuscript; Y.N. performed the majority of genetic analyses and analyzed the data; H.T. performed T-cell receptor analysis and designed q-PCR primers and probes; G.Y. contributed to the organization of software for linkage analysis and simulation; S.M. prepared the pooled DNA; M.O., K.M., Y.K, and Y.M. collected clinical data and specimens; T.T. and K.K. contributed to data analysis and interpretation, and to the writing of the article; S.O. and Y.A. supervised the entire project, designed and coordinated most of the experiments in this study, contributed to manuscript preparation, and are senior coauthors.

Conflict-of-interest disclosure: The authors declare no competing financial interests.

Correspondence: Seishi Ogawa, Department of Hematology and Oncology, Department of Regeneration Medicine for Hematopoiesis, The 21st Century COE Program, Graduate School of Medicine, University of Tokyo, 7-3-1, Hongo, Bunkyo-ku, Tokyo 113-8655, Japan; e-mail: sogawa-tky@umin.ac.jp; or Yoshiki Akatsuka, Division of Immunology, Aichi Cancer Center Research Institute, 1-1 Kanokoden, Chikusa-ku, Nagoya 464-8681, Japan; e-mail: yakatsuk@aichi-cc.jp.

References

1. Thomas ED Sr. Stem cell transplantation: past, present and future. Stem Cells. 1994;12:539-544.
2. Childs RW, Barrett J. Nonmyeloablative allogeneic immunotherapy for solid tumors. Annu Rev Med. 2004;55:459-475.
3. Goulmy E. Human minor histocompatibility antigens: new concepts for marrow transplantation and adoptive immunotherapy. Immunol Rev. 1997;157:125-140.
4. Bleakley M, Riddell SR. Molecules and mechanisms of the graft-versus-leukaemia effect. Nat Rev Cancer. 2004;4:371-380.
5. den Haan JM, Meadows LM, Wang W, et al. The minor histocompatibility antigen HA-1: a diallelic gene with a single amino acid polymorphism. Science. 1998;279:1054-1057.
6. Pierce RA, Field ED, Mutis T, et al. The HA-2 minor histocompatibility antigen is derived from a diallelic gene encoding a novel human class I myosin protein. J Immunol. 2001;167:3223-3230.
7. Akatsuka Y, Nishida T, Kondo E, et al. Identification of a polymorphic gene, BCL2A1, encoding two novel hematopoietic lineage-specific minor histocompatibility antigens. J Exp Med. 2003;197:1489-1500.
8. Warren EH, Vigneron NJ, Gavin MA, et al. An antigen produced by splicing of noncontiguous peptides in the reverse order. Science. 2006;313:1444-1447.
9. Kawase T, Akatsuka Y, Torikai H, et al. Alternative splicing due to an intronic SNP in HMSD generates a novel minor histocompatibility antigen. Blood. 2007;110:055-1063.
10. van Bergen CA, Kester MG, Jedema I, et al. Multiple myeloma-reactive T cells recognize an activation-induced minor histocompatibility antigen encoded by the ATP-dependent interferon-responsive (ADIR) gene. Blood. 2007;109:4089-4096.
11. Dolstra H, Fredrix H, Maas F, et al. A human minor histocompatibility antigen specific for B cell acute lymphoblastic leukemia. J Exp Med. 1999;189:301-308.
12. de Rijke B, van Horssen-Zoetbrood A, Beekman JM, et al. A frameshift polymorphism in P2X5 elicits an allogeneic cytotoxic T lymphocyte response associated with remission of chronic myeloid leukemia. J Clin Invest. 2005;115:3506-3516.
13. Brickner AG, Evans AM, Mito JK, et al. The PANE1 gene encodes a novel human minor histocompatibility antigen that is selectively expressed in B-lymphoid cells and B-CLL. Blood. 2006;107:3779-3786.
14. Warren EH, Otterud BE, Linterman RW, et al. Feasibility of using genetic linkage analysis to identify the genes encoding T cell-defined minor histocompatibility antigens. Tissue Antigens. 2002;59:293-303.
15. Consortium TIH. The International HapMap Project. Nature. 2003;426:789-796.
16. Consortium TIH. A haplotype map of the human genome. Nature. 2005;437:1299-1320.
17. Risch N, Merikangas K. The future of genetic studies of complex human diseases. Science. 1996;273:1516-1517.
18. Hirschhorn JN, Daly MJ. Genome-wide association studies for common diseases and complex traits. Nat Rev Genet. 2005;6:95-108.
19. Kennedy GC, Matsuzaki H, Dong S, et al. Large-scale genotyping of complex DNA. Nat Biotechnol. 2003;21:1233-1237.
20. Matsuzaki H, Dong S, Loi H, et al. Genotyping over 100 000 SNPs on a pair of oligonucleotide arrays. Nat Methods. 2004;1:109-111.
21. Barrett JC, Fry B, Maller J, Daly MJ. Haploview: analysis and visualization of LD and haplotype maps. Bioinformatics. 2005;21:263-265.
22. Parker KC, Bednarek MA, Coligan JE. Scheme for ranking potential HLA-A2 binding peptides based on independent binding of individual peptide side-chains. J Immunol. 1994;152:163-175.
23. Kubo RT, Sette A, Grey HM, et al. Definition of specific peptide motifs for four major HLA-A alleles. J Immunol. 1994;152:3913-3924.
24. Dolstra H, de Rijke B, Fredrix H, et al. Bi-directional allelic recognition of the human minor histocompatibility antigen HB-1 by cytotoxic T lymphocytes. Eur J Immunol. 2002;32:2748-2758.
25. Easton DF, Pooley KA, Dunning AM, et al. Genome-wide association study identifies novel breast cancer susceptibility loci. Nature. 2007;447:1087-1093.
26. Gudmundsson J, Sulem P, Manolescu A, et al.

Genome-wide association study identifies a second prostate cancer susceptibility variant at 8q24. Nat Genet. 2007;39:631-637.

27. Zeggini E, Weedon MN, Lindgren CM, et al. Replication of genome-wide association signals in UK samples reveals risk loci for type 2 diabetes. Science. 2007;316:1336-1341.
28. Su AI, Cooke MP, Ching KA, et al. Large-scale analysis of the human and mouse transcriptomes. Proc Natl Acad Sci U S A. 2002;99:4465-4470.
29. Nannya Y, Taura K, Kurokawa M, Chiba S, Ogawa S. Evolution of genome-wide power of genetic association studies based on empirical data from the HapMap project. Hum Mol Genet. 2007;16:3494-3505.
30. Spierings E, Brickner AG, Caldwell JA, et al. The minor histocompatibility antigen HA-3 arises from differential proteasome-mediated cleavage of the lymphoid blast crisis (Lbc) oncoprotein. Blood. 2003;102:621-629.
31. Brickner AG, Warren EH, Caldwell JA, et al. The immunogenicity of a new human minor histocompatibility antigen results from differential antigen processing. J Exp Med. 2001;193:195-206.
32. Kloosterboer FM, van Luxemburg-Heijs SA, van Soest RA, et al. Minor histocompatibility antigen-specific T cells with multiple distinct specificities can be isolated by direct cloning of IFNgamma-secreting T cells from patients with relapsed leukemia responding to donor lymphocyte infusion. Leukemia. 2005;19:83-90.
33. Tykodi SS, Warren EH, Thompson JA, et al. Allogeneic hematopoietic cell transplantation for metastatic renal cell carcinoma after nonmyeloablative conditioning: toxicity, clinical response, and immunological response to minor histocompatibility antigens. Clin Cancer Res. 2004;10:7799-7811.
34. Kenny JJ, Knobloch TJ, Augustus M, Carter KC, Rosen CA, Lang JC. GRS, a novel member of the Bcl-2 gene family, is highly expressed in multiple cancer cell lines and in normal leukocytes. Oncogene. 1997;14:997-1001.

Available online at www.sciencedirect.com
ScienceDirect
Cancer Letters 260 (2008) 137–145
CANCER Letters
www.elsevier.com/locate/canlet

Effective induction of anti-tumor immune responses with oligomannose-coated liposome targeting to intraperitoneal phagocytic cells

Yuzuru Ikehara [a,b,*], Nobumitsu Shiuchi [c], Sanae Kabata-Ikehara [a,b], Hayao Nakanishi [b], Naoaki Yokoyama [d], Hideaki Takagi [c], Toshi Nagata [e], Yukio Koide [e], Kiyotaka Kuzushima [f], Toshitada Takahashi [g], Kunio Tsujimura [e], Naoya Kojima [c]

[a] *Molecular Medicine Team of Research Center for Medical Glycoscience, National Institute of Advanced Industrial Science and Technology, Centeral 2-12, Room 211, 1-1-1 Umezono, Tsukuba, Japan*
[b] *Division of Oncological Pathology, Aichi Cancer Center Research Institute, Nagoya, Japan*
[c] *Department of Applied Biochemistry, The Institute of Glycotechnology, Tokai University, Hiratsuka, Japan*
[d] *Research Unit for Molecular Diagnosis, National Research Center for Protozoan Diseases, Obihiro University of Agriculture and Veterinary Medicine, Obihiro, Japan*
[e] *Department of Infectious Diseases, Hamamatsu University School of Medicine, Hamamatsu, Japan*
[f] *Division of Immunology, Aichi Cancer Center Research Institute, Nagoya, Japan*
[g] *Aichi Comprehensive Health Science Center of the Aichi Health Promotion Foundation, Aichi, Japan*

Received 2 July 2007; received in revised form 22 October 2007; accepted 29 October 2007

Abstract

We recently established a novel drug delivery system (DDS) using oligomannose-coated liposomes (OMLs) which are probably taken up by macrophages (Mϕ) to carry anti-cancer drugs to milky spots known as preferential metastatic sites of gastric cancers [Y. Ikehara, T. Niwa, L. Biao, S.K. Ikehara, N. Ohashi, T. Kobayashi, Y. Shimizu, N. Kojima, H. Nakanishi, A carbohydrate recognition-based drug delivery and controlled release system using intraperitoneal macrophages as a cellular vehicle, Cancer Res. 66 (2006) 8740–8748]. In the present study, we applied this intraperitoneal DDS for systemic cancer immunotherapy employing ovalbumin (OVA) as a model antigen. The cells taking up the OMLs containing FITC-OVA injected into the peritoneal cavity were predominantly Mϕ, as they showed adhesive characteristics and expressed F4/80 and CD11b almost exclusively. The phagocytic cells also took up bare OVA directly to the same extent as OML-enclosed OVA (OML-OVA), as it is a highly mannosilated protein. The phagocytic cells taking up OML-OVA, however, could activate OVA-specific $CD8^+$ (from OT-I: H-$2K^b$/$OVA_{257-264}$-specific) and $CD4^+$ (from OT-II: H-$2A^b$/$OVA_{323-339}$-specific) T cells much more effectively *in vitro* than those taking up bare OVA. Furthermore, only the mice pre-immunized with OML-OVA rejected E.G7-OVA (OVA-transfected EL4) but not EL4. These results indicate that

* Corresponding author. Address: Molecular Medicine Team of Research Center for Medical Glycoscience, National Institute of Advanced Industrial Science and Technology, Tsukuba, Japan. Tel.: +81 29 861 5853; Fax: +81 29 861 3462.
E-mail address: yuzuru-ikehara@aist.go.jp (Y. Ikehara).

0304-3835/$ - see front matter
doi:10.1016/j.canlet.2007.10.038

the OMLs can also be used as an effective antigen delivery system for cancer immunotherapy activating both CTL and Th subsets.

Keywords: Drug delivery system; Cancer vaccine; Immune responses to cancer; Oligomannose liposome

1. Introduction

While recent advances in tumor immunology enable us to identify tumor antigens recognized by T cells and understand the molecular and cellular bases of T cell-mediated anti-tumor responses, the clinical realization of effective immunotherapy for solid tumors has not yet been convincingly achieved [1,2]. Many $CD8^+$ and $CD4^+$ T cells recognizing tumor antigen in the context of MHC class I and II, respectively, have been reported, and the former are known to be a major effector of the adaptive anti-tumor immune responses [3–5]. $CD4^+$ T cells play an important role for the expansion and persistence of $CD8^+$ T cells, while some of them are known to function as regulatory cells [5–7]. Optimal anti-tumor immune responses are therefore considered to require the concomitant activation of both $CD8^+$ and $CD4^+$ T cells and the selective activation of $CD4^+$ T cells with helper but not regulatory functions [8]. Endogenous and exogenous antigens are presented as peptides preferentially by MHC class I and II, respectively, and most tumor antigen peptides are derived from the proteins expressed endogenously. Novel methods to make tumor antigens presented simultaneously by both MHC class I and II molecules are therefore needed for the concomitant activation of antigen-specific $CD8^+$ and $CD4^+$ T cells, and many attempts have been made for this purpose [2,3,8].

We recently developed a novel drug delivery system (DDS) using oligomannose-coated liposomes (OMLs) [9,10] which are effectively taken up by $F4/80^+$ intraperitoneal cells to carry anti-cancer drugs to milky spots known as a preferential metastatic site of gastric and ovarian cancers [9,11,12]. We demonstrated that this system could control the formation of overt metastasis of seeded gastric cancer cells at the extra-nodal lymphoid tissues such as the omentum [10].

In the present study, we applied this OML-based intraperitoneal DDS for cancer immunotherapy using ovalbumin (OVA) as a model antigen, aiming at the concomitant activation of antigen-specific $CD8^+$ and $CD4^+$ T cells. Peritoneal phagocytic cells took up OML containing OVA and then migrated into milky spots as previously reported. In addition, they activated both OVA-specific $CD8^+$ [13,14] and $CD4^+$ [15] T cells effectively *in vitro*. Spleen cells from OML-enclosed OVA (OML-OVA)-injected mice showed an effective killing activity against E.G7-OVA (OVA-transfected EL4) [16] but not EL4 [17] *in vitro*, and only the mice pre-immunized with OML-OVA rejected E.G7-OVA but not EL4 *in vivo*. In light of these results obtained *in vitro* and *in vivo*, the potential of our novel OML-based immunization method for the prevention of tumor metastasis is discussed.

2. Materials and methods

2.1. Mice

Female C57BL/6 (B6) mice ($H\text{-}2^b$) at 8–12 weeks of age were obtained from Charles River Japan Inc. (Yokohama, Japan) and kept under standard housing conditions. T cell receptor transgenic mice OT-I (specific for $H\text{-}2K^b/OVA_{257\text{–}264}$) [13,14] and OT-II ($H\text{-}2A^b/OVA_{323\text{–}339}$) [15] were obtained from the Jackson Laboratory (Bar Harbor, ME) and maintained under specific pathogen-free conditions. All animal experiments were performed under the experimental protocol approved by the Ethics Review Committee for Animal Experimentation of Aichi Cancer Center.

2.2. Cell lines

EL4 [17], a B6-derived thymoma cell line, was maintained in RPMI1640 medium (Invitrogen, Carlsbad, CA) supplemented with 8% fetal bovine serum, 0.2% L-glutamine, 100 U/ml penicillin, 100 μg/ml streptomycin, 0.1% Hepes, 0.1 mM non-essential amino acids, 1 mM sodium pyruvate, and 50 μM 2-ME (complete RPMI). EG.7-OVA (EL4 transfected with *OVA* gene) [16] was obtained from ATCC (Manassas, VA) and maintained in complete RPMI supplemented with 400 μg/ml G418 (Wako, Osaka, Japan) in a humidified 5% CO_2 incubator at 37 °C.

2.3. Man3-DPPE and liposome preparation

Dipalmitoylphosphatidylcholine (DPPC), cholesterol, and dipalmitoylphosphatidylethanolamine (DPPE) were purchased from Sigma–Aldrich (St. Louis, MO). Mannotriose (Man3: Manα1-6(Manα1-3)Man) was purchased from Funakoshi Co., Ltd. (Tokyo, Japan). Man3-DPPE was prepared by conjugation of the mannotriose with DPPE by reductive amination as described in previous papers [10,18]. The purity of Man3-DPPE was confirmed by high-performance thin-layer chromatography (Silica gel 60 HPTLC plate, MERCK, Darmstadt, Germany) and time-of-flight mass spectrometry (Auto FLEX, Bruker Daltonics, Bremen, Germany). The purified Man3-DPPE was quantified by determination of the phosphate contained.

Liposomes were prepared as described previously [10]. Briefly, a chloroform–methanol (2:1, v/v) solution containing 1.5 μmol of DPPC and 1.5 μmol of cholesterol was placed in a conical flask and dried by rotary evaporation. Subsequently, 2 ml ethanol containing 0.15 μmol of Man3-DPPE was added to the flask and evaporated to prepare a lipid film containing neoglycolipids. Procedures for protein-encasing of oligomannose-coated liposomes (OMLs) were performed as described previously [10]. The multilamellar vesicles were generated with either 200 μl of FITC-labelled or non-labelled OVA (5.0 mg/ml, Sigma–Aldrich), Alexa Fluor 680 (Molecular Probes, Eugene, OR)-labelled bovine serum albumin (BSA, 5 mg/ml, Sigma–Aldrich), or PBS in the dried lipid film by intense vortex dispersion. The multilamellar vesicles were extruded 10 times through polycarbonate membranes of 1 μm pore (Nucleopore, Pleasanton, CA). Liposomes entrapping proteins were separated from free untrapped proteins by four successive rounds of washing in PBS with centrifugation (20,000*g*, 30 min) at 4 °C. The amounts of entrapped proteins were measured using a modified Lowry protein assay reagent (Pierce, Rockford, IL) in the presence of 0.3% (w/v) sodium dodecyl sulfate using BSA as the standard.

2.4. Flow cytometry

One hour after intraperitoneal injection, peritoneal exudate cells (PEC) were recovered from B6 mice with 5 ml ice cold PBS. PEC were incubated on ice for 30 min with fluorescein-labelled antibodies against mouse hematopoietic cell lineage markers after blocking with mouse Fc Blocker (BD Biosciences, San Jose, CA) and then analysed on a FACS Calibur (BD Biosciences). The following monoclonal antibodies used in this study were purchased or kindly provided: anti-F4/80 (A3-1, Serotec Ltd., Oxford, UK), anti-MHC class II (M5/114.15.2, e-Bioscience, Boston, MA), anti-CD11b (M1/70.15, Caltag Laboratories, Burlingame, CA), anti-CD3ε (145-2C11, BD Biosciences), anti-CD19 (1D3, BD Biosciences), and anti-H-2K^{b}D^b (20-8-4S, Dr. E. Nakayama, Okayama University).

2.5. Macrophage depletion by plastic adhesion

PEC suspension (2×10^7 cells in 10 ml of complete RPMI) was poured into a 75 cm^2 tissue culture flask and incubated at 37 °C for 2 h in a humidified 5% CO_2 incubator. Non-adherent cells were collected with serum-free DMEM and subjected to FACS analysis.

2.6. In vitro activation of OVA-specific T cells

One hour after injection of either OML-encased OVA or bare OVA into the peritoneal cavity of B6 mice, PEC were recovered with 5 ml ice cold PBS. The PEC suspended in complete RPMI were seeded into a 96-well culture plate (5×10^5 cells in each well) and incubated at 37 °C for overnight in a humidified 5% CO_2 incubator. On the next day, non-adherent cells were washed out with complete RPMI, and co-cultured with 5×10^5 cells of either CD8$^+$ or CD4$^+$ T cells from the spleen of OT-I and OT-II mice, respectively. CD8$^+$ and CD4$^+$ T cells were prepared with the isolation kits for corresponding subsets (Miltenyi Biotec Inc., Auburn, CA). The supernatants were collected at 24, 48, and 72 h and assayed for IFN-γ production with Mouse IFN-γ ELISA kit (Pierce Biotechnology, Inc., Rockford, IL).

2.7. CTLs assay

B6 mice were immunized biweekly three times by intraperitoneal injection of 1 μg OVA in liposome/mouse with or without oligomannose coating. Spleen cells were isolated from the mice 1 week after the last challenge, and 1×10^6 spleen cells were stimulated with 10 μg OVA in 1 ml for 72 h. The effector cells thus prepared were co-cultured with target cells (E.G7-OVA or EL4) at various effector/target ratios for 8 h at 37 °C, and the cytotoxicity was measured with CytoTox96 Non-Radioactive Cytotoxicity assay kit (Promega, Madison, WI).

2.8. Tumor assay

Tumor cells (in 0.2 ml) were injected intradermally into the backs of mice with a 27 gauge needle. The diameter of the tumors was measured with Vernier calipers twice at right angles to calculate the mean diameter, and the survival time after tumor challenges was followed.

3. Results

3.1. OMLs are taken up preferentially by intraperitoneal macrophages

We showed that neoglycolipid-coated liposomes are ingested by intraperitoneal cells much more effectively than non-coated liposomes [10]. Of those, OMLs are incorporated most effectively, and the cells ingesting

OMLs are preferentially F4/80$^+$ and migrate into extranodal lymphoid tissues in the omentum after the uptake. We have also shown that the OML-ingesting cells are very useful drug delivery vehicles for cancer chemotherapy in the previous study [9,10]. To verify whether the OMLs are applicable also for cancer immunotherapy, we first analyzed in detail the peritoneal cells incorporating OMLs. Bovine serum albumin (BSA, Sigma–Aldrich) was labelled with Alexa Fluor 680, encased in OML and then injected into the peritoneal cavity of B6 mice. One hour after the injection of OMLs containing Alexa Fluor 680-labelled BSA, PEC were collected and analyzed. As shown in Fig. 1A, PEC were divided into three groups based on the incorporation of OMLs. When adherent cells were removed by plastic dish adherence, only the population with higher OML uptake (R1) disappeared (Fig. 1B). In addition, most cells of R1 express F4/80 and CD11b but not CD3 and CD19 (Fig. 1C), suggesting that R1 population preferentially consists of macrophages (Mϕ). The PEC with lower OML uptake (R2) did not express F4/80, and nearly 2/3 of them were considered to be B cells because of their CD19 expression. These results together confirmed that OMLs injected into the peritoneal cavity were ingested preferentially by Mϕ, and also indicate that OML is a good vehicle for the phagocytosis of non-glycosylated proteins.

3.2. Phagocytic cells ingesting OMLs activate both CD8 and CD4 T cells in vitro in an antigen-specific manner

We next analyzed the antigen-presenting capacity of the phagocytic cells ingesting OMLs containing ovalbumin (OVA) as an antigen. CD8$^+$ T cells from OT-I (a transgenic strain of T cell receptor (TCR) recognizing $OVA_{257-264}$ peptide presented by H-2K^b) and CD4$^+$ T cells from OT-II (a transgenic strain of TCR recognizing $OVA_{323-339}$ peptide presented by H-2A^b) were used as responder cells. When these T cells were co-cultured with adherent cells enriched from PEC of the mouse intraperitoneally injected with OML-encased OVA (OML-OVA), both CD8$^+$ and CD4$^+$ T cells produced large amounts of IFN-γ (Fig. 2). Though adherent cells from the mice injected with soluble OVA also stimulated both CD8$^+$ and CD4$^+$ T cells, much higher amounts of OVA were needed compared to those from the mice injected with OML-OVA. Mϕ ingesting OML-OVA are supposed to

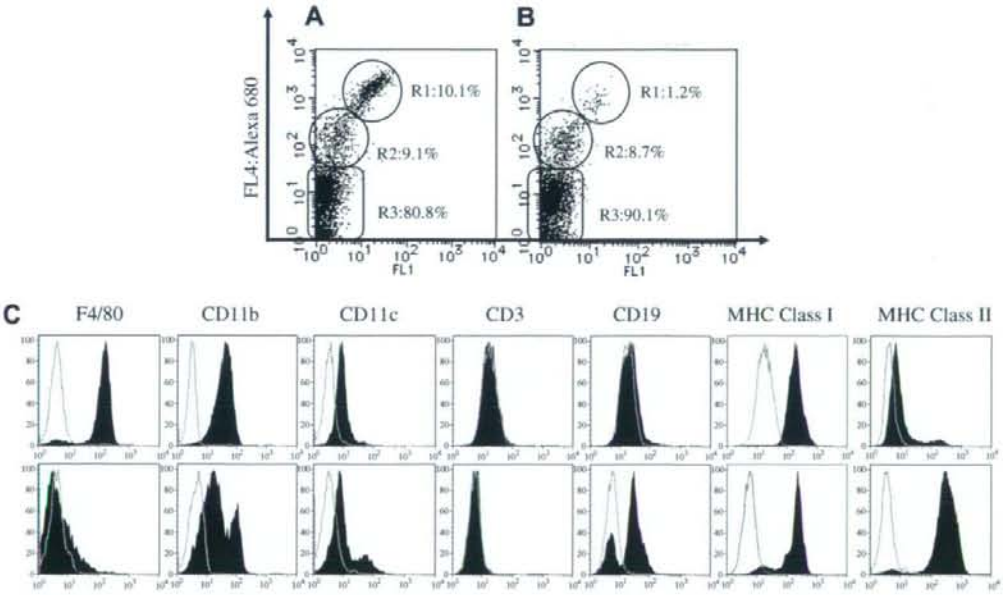

Fig. 1. OMLs injected into the peritoneal cavity were ingested preferentially by adhesive cells. One hour after injection of OMLs containing Alexa Fluor 680-labelled BSA, PEC were collected and their fluorescence was analyzed by flow cytometry (A). Non-adherent PEC were further isolated by plastic adherence for 2 h and analyzed (B). (C) Phenotypic analysis of PEC derived from OML-injected mice. One hour after injection of OMLs containing Alexa Fluor 680-labelled OVA, PEC were collected and stained with mAbs indicated. As shown in (A) and (B), PEC were divided into three groups based on their fluorescence intensity of Alexa Fluor 680, and the surface phenotypes of R1 and R2 were further analyzed.

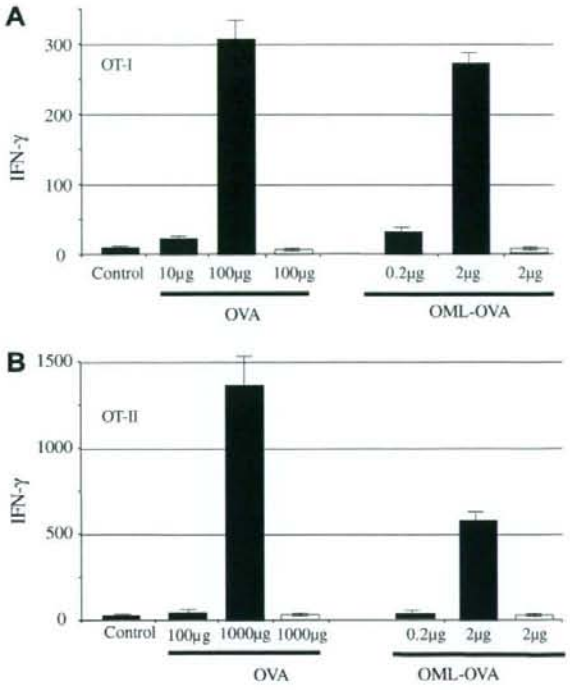

Fig. 2. Mϕ ingesting OVA encased in OML activate OVA-specific $CD8^+$ and $CD4^+$ T cells much more effectively than those ingesting soluble OVA. One hour after intraperitoneal injection of antigens, PEC were prepared from mice, and adherent cells were enriched by plastic adherence. $CD8^+$ and $CD4^+$ T cells were purified from spleen of OT-I (A) and OT-II (B), respectively, co-cultured (closed bar) with adherent PEC or cultured adherent PEC alone (open bar) for 24 h, and then production of IFN-γ in supernatants was tested by ELISA. PEC recovered from mice without any treatment was used as control. OML-OVA, OVA encased in OML; OVA, OVA; control, OML containing PBS. The graph shows the average and standard error from three independent experiments.

present antigen effectively also *in vivo*, as they effectively induced proliferation responses of OVA-specific $CD8^+$ T cells in the spleens of OT-I mice (Supplement Figure 1).

We next analyzed the uptake efficiency of OML-encased and soluble OVA and found that peritoneal phagocytic cells effectively uptake OVA irrespective of sugar encapsulation (Fig. 3). The uptake of soluble OVA is probably mediated by mannose receptors, as it is known as a highly mannosylated protein [19]. These results together indicate that OML-mediated ingestion promotes the presentation of OVA peptides by both MHC class I and II molecules by enhancing the antigen processing but not the uptake efficiency.

3.3. Induction of antigen-specific cytotoxic T lymphocytes (CTL) in vitro by OML-mediated immunization

We next performed CTL assay to detect OVA-specific T cells in the spleen. Only the spleen cells from mice immunized with OML-OVA but not bare liposome (BL)-encased OVA showed cytotoxicity against E.G7-OVA. The spleen cells from neither group showed cytotoxicity against EL4, confirming that OVA-specific CTL can be effectively induced *in vivo* by OML-OVA immunization (Fig. 4).

3.4. OML-mediated immunization induces antigen-specific anti-tumor immunity in vivo

We finally examined whether intraperitoneal immunization with OMLs also induces antigen-specific anti-tumor immunity *in vivo*. Mice were immunized intraperitoneally with OVA with or without OML encasing and then challenged with E.G7-OVA or EL4. As shown in Fig. 5, only the mice immunized with OML-OVA survived for more than 70 days when challenged with E.G7-OVA, while naïve and bare OVA-immunized mice died within 55 days. All the mice including those immunized with OML-OVA died within 30 days when challenged with EL4, indicating that the rejection of

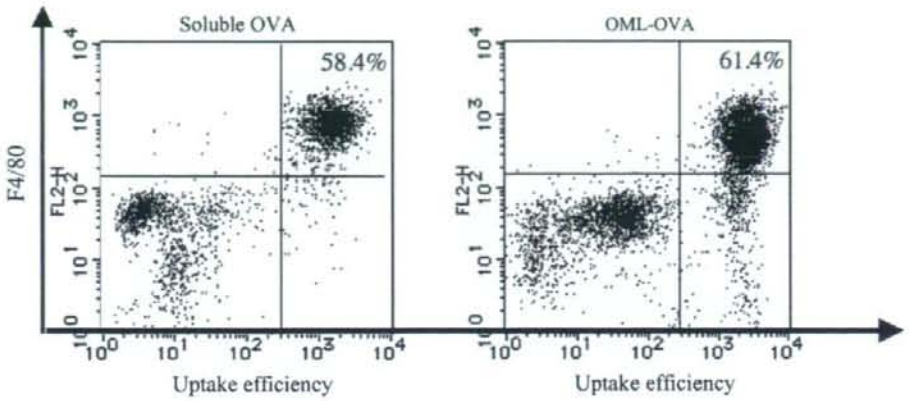

Fig. 3. Peritoneal F4/80$^+$ cells uptake OVA effectively irrespective of carbohydrate encapsulation. One hour after injection of either soluble FITC-OVA (20 μg) or OML-encapsulated FITC-OVA (20 μg) into the peritoneal cavity of B6 mice, uptake efficiency of FITC-OVA by peritoneal cells was analyzed by flow cytometry together with F4/80 expression.

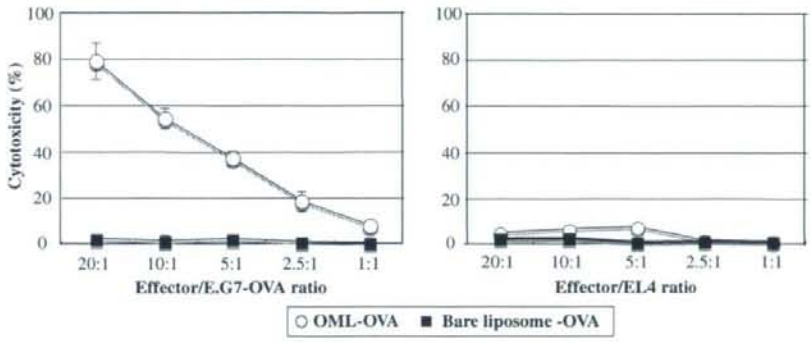

Fig. 4. OML-OVA-generated OVA-specific cytotoxicity. B6 mice were immunized biweekly three times by intraperitoneal injection of 1 μg OVA encased in oligomannose-coated (OML-OVA, open symbols) or bare liposomes (bare liposome-OVA, closed symbols). Spleen cells were isolated from mice one week after the last challenge, and 1×10^6 cells were stimulated with 10 μg OVA in 1 ml for 72 h. The graph shows the average and standard error from three independent experiments.

E.G7-OVA is OVA-specific. These results together showed that OML-mediated immunization can induce systemic immune response robust enough to protect mice from tumor challenge in an antigen-specific manner.

4. Discussion

In this study, we demonstrated that our novel OML-based drug delivery system (DDS) targeted to intraperitoneal phagocytic cells can also be used for the induction of systemic immune responses. After ingesting OML-encased OVA (OML-OVA), intraperitoneal phagocytic cells to extra-nodal lymphoid tissues in abdominal cavity and presented OVA-derived peptides in the context of both MHC class I and II molecules. Only the mice pre-immunized with OML-OVA rejected E.G7-OVA but not EL4 challenged subcutaneously. These results together indicate that the OMLs can be used as an effective antigen delivery system for immunotherapy activating both CTL and Th subsets. Fig. 6 shows the plausible induction process of anti-tumor immunity starting from phagocytic cells triggered by OML injection.

OMLs are very useful not only for the promotion of non-glycosylated protein uptake by antigen-presenting cells but also for the enhancement of antigen-processing of encased antigens. Endogenous

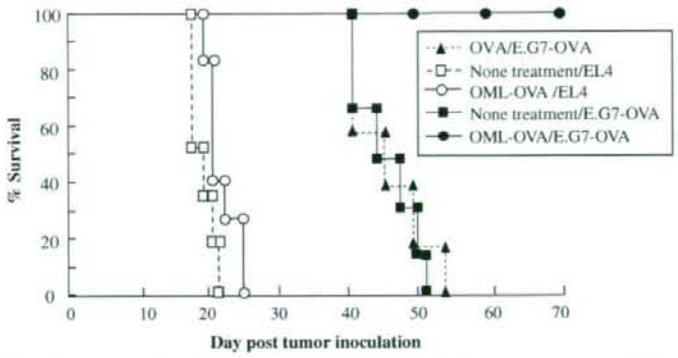

Fig. 5. OML-mediated immunization induces antigen-specific anti-tumor immunity *in vivo*. OML-OVA-immunized (circles) and naïve (squares) mice were challenged with E.G7-OVA (closed circles and squares) or EL4 cells (open circles and squares). As a control, mice were immunized with soluble OVA and challenged with E.G7-OVA (closed triangles).

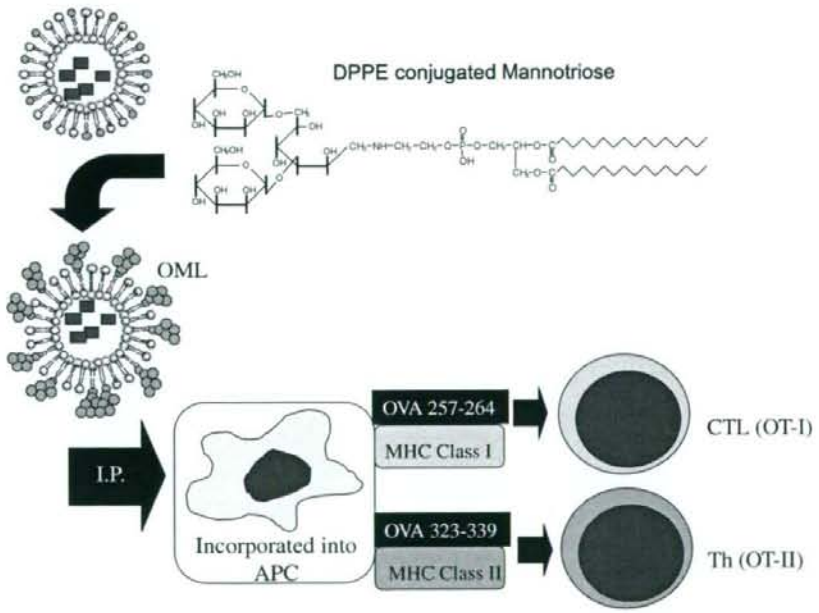

Fig. 6. Possible mechanism of OML-based vaccine delivery. Coating of bare liposomes with DPPE-conjugated mannotriose facilitates functions of intraperitoneal macrophages, resulting in antigen-specific activation of both CTL and Th populations.

and exogenous antigens are presented preferentially by MHC class I and II, respectively. OML-OVA, however, were effectively directed to both pathways, even when added exogenously. This advantage of OML-mediated immunization will hopefully facilitate the simultaneous activation of tumor antigen-specific $CD4^+$ and $CD8^+$ T cells as shown here with OVA. It is also very interesting to study the mechanism by which OML-mediated ingestion of antigens enhances the antigen presentation by both MHC molecules [20–22]. So far, we observed the up-regulation of CD80 and CD86 on OML-ingesting cells (in press on Cytokine, H. Takagi et al.), but it seems very important to know the additional signals to

make antigen presenting cells more immunogenic [23]. Additional adjuvant effects of various cytokines and/or toll-like receptor ligands on OML-mediated immunization are now being investigated.

Another advantage of OML-mediated immunization is Th1-skewing of the cytokine profiles. Indeed, OT-I and OT-II T cells stimulated with antigen-presenting cells ingesting OML-OVA produced IFN-γ but not IL-4 or IL-10 (unpublished observation). Moreover, our previous study demonstrated that the OML-mediated immunization protects BALB/c mice against *Leishmania major* infection, possibly due to the Th1-skewing of immune responses [24]. We observed that phagocytic cells ingesting OML preferentially produce IL-12 (unpublished observation), suggesting this cytokine is a key of Th1-skewing as reported previously [25]. Further investigation of the mechanism of this Th1-skewing of immune responses induced by OML-mediated immunization is currently underway.

Cells belonging to the monocyte-Mϕ lineage have been known to be heterogeneous, reflecting the plasticity and versatility of these cells in response to various microenvironmental signals [26]. Mϕ are now roughly categorized into M1 and M2 based on their functional properties, and several studies revealed that M1 and M2 promote type I and type II Th responses, respectively [27–29]. It is also reported that M1 and M2 are prone to induce inflammatory and immunoregulatory responses, respectively [29]. A possible concern of our DDS system is therefore the protumoral effects by M2 with antigen-encased OMLs, as they are supposed to express macrophage mannose receptors induced by IL-4 [30]. Although at least our *in vitro* study clearly showed OML-mediated skewing to type I immune responses, more precise investigation including the conditions for M1 polarization should be done especially in tumor-bearing mice. In addition, characteristics of the small population of non-Mϕ cells ingesting OMLs should be investigated as well.

In order to use our DDS in clinical study, the best administration routes should be determined to pursue repetitive vaccination while avoiding possible side effects. As generally acknowledged, intraperitoneal administration is accompanied with a high risk of side effects such as catheter-related complications, and abdominal pain [31]. In this connection, we have already obtained anti-tumor effects by subcutaneous injection of OML-OVA similar to those by intraperitoneal injection. However, side effects induced by subcutaneous injection of OMLs should be further investigated to assure their safe clinical application.

In the previous study, we reported that the formation of intraperitoneal metastasis of seeded gastric cancer cells in milky spots can be controlled with OMLs containing anti-cancer drugs [10]. In the present study, we have further extended the possibility of OMLs for the immunotherapy of systemic metastasis and existing tumor cells aside from milky spots. Oligomannose coating of liposomes showed the best uptake efficiency by intraperitoneal Mϕ among the neoglycolipids so far tested, and the encased antigen was effectively presented by both MHC class I and II molecules. However, the additional effects for immune responses by other neoglicolipids (shown here) have not been studied at all so far. We have a great interest in their effects on immune responses and are seeking sugar materials with immunoregulatory properties. If such materials are found, we believe that further study of our sugar-coated liposome technology will find it also to be applicable for antigen-specific regulation of autoimmune diseases and allergy.

Acknowledgments

We thank Ms. Y. Matsudaira and Ms. K. Nishida for their excellent technical assistance. This work was supported by the Industrial Technology Research Grant Program in 04' from the New Energy and Industrial Technology Development Organization (NEDO) of Japan, and in part by a grant for Hi-tech research program from Tokai University and by the Program for Promotion of Basic Research Activities for Innovative Biosciences (PROBRAIN). The costs of publication of this article were defrayed in part by the payment of page charges. This article must therefore be hereby marked advertisement in accordance with 18 U.S.C. Section 1734 solely to indicate this fact.

Appendix A. Supplementary data

Supplementary data associated with this article can be found, in the online version, at doi:10.1016/j.canlet.2007.10.038.

References

[1] L. Gattinoni, D.J. Powell Jr., S.A. Rosenberg, N.P. Restifo, Adoptive immunotherapy for cancer: building on success, Nat. Rev. Immunol. 6 (2006) 383–393.

[2] S.A. Rosenberg, J.C. Yang, N.P. Restifo, Cancer immunotherapy: moving beyond current vaccines, Nat. Med. 10 (2004) 909–915.
[3] S.A. Rosenberg, Progress in the development of immunotherapy for the treatment of patients with cancer, J. Intern. Med. 250 (2001) 462–475.
[4] T. Boon, P.G. Coulie, B.J. Van den Eynde, P. van der Bruggen, Human T cell responses against melanoma, Annu. Rev. Immunol. 24 (2006) 175–208.
[5] D.M. Pardoll, S.L. Topalian, The role of CD4+ T cell responses in antitumor immunity, Curr. Opin. Immunol. 10 (1998) 588–594.
[6] R.F. Wang, G. Peng, H.Y. Wang, Regulatory T cells and toll-like receptors in tumor immunity, Semin. Immunol. 18 (2006) 136–142.
[7] S. Sakaguchi, R. Setoguchi, H. Yagi, T. Nomura, Naturally arising Foxp3-expressing CD25+CD4+ regulatory T cells in self-tolerance and autoimmune disease, Curr. Top. Microbiol. Immunol. 305 (2006) 51–66.
[8] A.M. Leen, C.M. Rooney, A.E. Foster, Improving T cell therapy for cancer, Annu. Rev. Immunol. 25 (2007) 243–265.
[9] Y. Ikehara, N. Kojima, Development of a novel oligomannose-coated liposome-based anticancer drug-delivery system for intraperitoneal cancer, Curr. Opin. Mol. Ther. 9 (2007) 53–61.
[10] Y. Ikehara, T. Niwa, L. Biao, S.K. Ikehara, N. Ohashi, T. Kobayashi, Y. Shimizu, N. Kojima, H. Nakanishi, A carbohydrate recognition-based drug delivery and controlled release system using intraperitoneal macrophages as a cellular vehicle, Cancer Res. 66 (2006) 8740–8748.
[11] L.F. Krist, M. Kerremans, D.M. Broekhuis-Fluitsma, I.L. Eestermans, S. Meyer, R.H. Beelen, Milky spots in the greater omentum are predominant sites of local tumour cell proliferation and accumulation in the peritoneal cavity, Cancer Immunol. Immunother. 47 (1998) 205–212.
[12] A. Hagiwara, T. Takahashi, K. Sawai, H. Taniguchi, M. Shimotsuma, S. Okano, C. Sakakura, H. Tsujimoto, K. Osaki, S. Sasaki, et al., Milky spots as the implantation site for malignant cells in peritoneal dissemination in mice, Cancer Res. 53 (1993) 687–692.
[13] K.A. Hogquist, S.C. Jameson, W.R. Heath, J.L. Howard, M.J. Bevan, F.R. Carbone, T cell receptor antagonist peptides induce positive selection, Cell 76 (1994) 17–27.
[14] S.R. Clarke, M. Barnden, C. Kurts, F.R. Carbone, J.F. Miller, W.R. Heath, Characterization of the ovalbumin-specific TCR transgenic line OT-I: MHC elements for positive and negative selection, Immunol. Cell Biol. 78 (2000) 110–117.
[15] M.J. Barnden, J. Allison, W.R. Heath, F.R. Carbone, Defective TCR expression in transgenic mice constructed using cDNA-based alpha- and beta-chain genes under the control of heterologous regulatory elements, Immunol. Cell Biol. 76 (1998) 34–40.
[16] M.W. Moore, F.R. Carbone, M.J. Bevan, Introduction of soluble protein into the class I pathway of antigen processing and presentation, Cell 54 (1988) 777–785.
[17] P.A. Gorer, Studies in antibody response of mice to tumour inoculation, Br. J. Cancer 4 (1950) 372–379.
[18] T. Mizuochi, R.W. Loveless, A.M. Lawson, W. Chai, P.J. Lachmann, R.A. Childs, S. Thiel, T. Feizi, A library of oligosaccharide probes (neoglycolipids) from *N*-glycosylated proteins reveals that conglutinin binds to certain complex-type as well as high mannose-type oligosaccharide chains, J. Biol. Chem. 264 (1989) 13834–13839.
[19] T. Tai, K. Yamashita, M. Ogata-Arakawa, N. Koide, T. Muramatsu, S. Iwashita, Y. Inoue, A. Kobata, Structural studies of two ovalbumin glycopeptides in relation to the endo-beta-*N*-acetylglucosaminidase specificity, J. Biol. Chem. 250 (1975) 8569–8575.
[20] M.C. Tan, A.M. Mommaas, J.W. Drijfhout, R. Jordens, J.J. Onderwater, D. Verwoerd, A.A. Mulder, A.N. van der Heiden, T.H. Ottenhoff, M. Cella, A. Tulp, J.J. Neefjes, F. Koning, Mannose receptor mediated uptake of antigens strongly enhances HLA-class II restricted antigen presentation by cultured dendritic cells, Adv. Exp. Med. Biol. 417 (1997) 171–174.
[21] A. Lanzavecchia, Mechanisms of antigen uptake for presentation, Curr. Opin. Immunol. 8 (1996) 348–354.
[22] F. Sallusto, M. Cella, C. Danieli, A. Lanzavecchia, Dendritic cells use macropinocytosis and the mannose receptor to concentrate macromolecules in the major histocompatibility complex class II compartment: downregulation by cytokines and bacterial products, J. Exp. Med. 182 (1995) 389–400.
[23] J.S. Lam, M.K. Mansour, C.A. Specht, S.M. Levitz, A model vaccine exploiting fungal mannosylation to increase antigen immunogenicity, J. Immunol. 175 (2005) 7496–7503.
[24] Y. Shimizu, K. Yamakami, T. Gomi, M. Nakata, H. Asanuma, T. Tadakuma, N. Kojima, Protection against *Leishmania major* infection by oligomannose-coated liposomes, Bioorg. Med. Chem. 11 (2003) 1191–1195.
[25] G. Trinchieri, Interleukin-12 and the regulation of innate resistance and adaptive immunity, Nat. Rev. Immunol. 3 (2003) 133–146.
[26] F.O. Martinez, S. Gordon, M. Locati, A. Mantovani, Transcriptional profiling of the human monocyte-to-macrophage differentiation and polarization: new molecules and patterns of gene expression, J. Immunol. 177 (2006) 7303–7311.
[27] S. Gordon, Alternative activation of macrophages, Nat. Rev. Immunol. 3 (2003) 23–35.
[28] A. Mantovani, A. Sica, M. Locati, Macrophage polarization comes of age, Immunity 23 (2005) 344–346.
[29] A. Mantovani, A. Sica, S. Sozzani, P. Allavena, A. Vecchi, M. Locati, The chemokine system in diverse forms of macrophage activation and polarization, Trends Immunol. 25 (2004) 677–686.
[30] M. Stein, S. Keshav, N. Harris, S. Gordon, Interleukin 4 potently enhances murine macrophage mannose receptor activity: a marker of alternative immunologic macrophage activation, J. Exp. Med. 176 (1992) 287–292.
[31] S.A. Cannistra, Intraperitoneal chemotherapy comes of age, N. Engl. J. Med. 354 (2006) 77–79.

European Journal of Haematology ISSN 0902-4441

ORIGINAL ARTICLE

Low absolute lymphocyte count is a poor prognostic marker in patients with diffuse large B-cell lymphoma and suggests patients' survival benefit from rituximab

Yasuhiro Oki, Kazuhito Yamamoto, Harumi Kato, Yachiyo Kuwatsuka, Hirofumi Taji, Yoshitoyo Kagami, Yasuo Morishima

Department of Hematology and Cell Therapy, Aichi Cancer Center Hospital, Nagoya, Japan

Abstract

Objectives: To evaluate the prognostic value of absolute lymphocyte count (ALC) at diagnosis in patients with diffuse large B-cell lymphoma (DLBCL). *Methods:* In a large cohort of patients with DLBCL treated with CHOP ($n = 119$) or RCHOP ($n = 102$) in our institution, we evaluated the prognostic value of ALC at diagnosis with regards to treatment response, overall (OS) and progression-free survival (PFS). Use of rituximab, all International Prognostic Index (IPI) determinants, β2microglobulin level, presence of B symptoms or bulky disease, and ALC were evaluated. *Results:* Low ALC ($<1.0 \times 10^9$/L) was associated with advanced stage, performance status ≥2, elevated lactate dehydrogenase, number of extranodal involvement ≥2, B symptoms, elevated β2microglobulin and higher IPI risk group. Low ALC was associated with lower CR rate by univariate analysis (odds ratio = 3.29, $P = 0.024$) but not by multivariate analysis. By univariate analysis using Cox proportional hazard model, low ALC was associated with shorter OS [hazard ratio (HR) = 2.89, $P < 0.001$] and PFS (HR = 2.91, $P < 0.001$). Multivariate analysis revealed that low ALC was associated with shorter OS (HR = 2.51, $P = 0.003$) and PFS (HR = 2.72, $P < 0.001$), independent of above-mentioned parameters. Subclass analyses revealed that the use of rituximab improves OS in patients with low ALC (HR = 0.42, $P = 0.05$) but not in those with high ALC (HR = 0.83, $P = 0.71$). This observation was most obvious in patients with higher IPI score. *Conclusion:* Low ALC is a poor prognostic marker in patients with DLBCL and suggests patients' survival benefit from rituximab.

Key words absolute lymphocyte count; diffuse large B-cell lymphoma; prognostic factor; rituximab

Correspondence Yasuhiro Oki, MD, Department of Hematology and Cell Therapy, Aichi Cancer Center Hospital, 1-1 Kanokoden, Chikusa-ku, Nagoya 464-8681, Japan. Tel: +81-52-762-6111; Fax: +81-52-764-2967; e-mail: yooki-tky@umin.ac.jp

Accepted for publication 14 July 2008

doi:10.1111/j.1600-0609.2008.01129.x

Prognostication of patients with diffuse large B-cell lymphoma (DLBCL) is important in determining optimal treatment approaches. Numbers of prognostic factors have been studied, but some require expensive molecular testing and thus not clinically applicable. Inexpensive and readily available prognostic factors are practical and helpful.

Low absolute lymphocyte count (ALC) at diagnosis is associated with poor prognosis in patients with advanced Hodgkin lymphoma (1) as well as follicular lymphoma (2). A recent preliminary study with short follow-up duration also suggested a potential prognostic value of ALC in DLBCL (3). While International Prognostic Index (IPI) is currently the most valuable prognostic indicator in patients with aggressive lymphoma, ALC was not included in the parameters analyzed (4). We performed a retrospective study evaluating the prognostic value of low ALC using our large cohort of patients with DLBCL, about half treated with CHOP and the rest with RCHOP.

Patients and methods

This retrospective study was approved by the institutional review board. We reviewed 221 consecutive newly

diagnosed patients with non-HIV-associated DLBCL who were treated with CHOP (n = 119; before approval of rituximab) or RCHOP (n = 102; after approval) based therapy at Aichi Cancer Center Hospital between January 1999 and January 2007. Age (≤60 or >60), performance status (PS, ≤1 or ≥2), B symptoms (present or absent), stage (≤2 or ≥3), number of extranodal involvement (≤1 or ≥2), bulky disease (largest diameter of the disease ≥10 cm, present or absent) serum lactate dehydrogenase (LDH) levels (normal or elevated), ALC at diagnosis, IPI group (scored from 0 to 5 by age >60, stage ≥3, PS ≥2, LDH higher than upper limit of normal range and number of extranodal involvement ≥2, and risk groups were classified as low by score 0/1, low-intermediate by score 2, high-intermediate by score 3 and high by score 4/5), initial treatment (CHOP or RCHOP) were collected and incorporated as potential prognostic factors in various analyses. Serum β2microglobulin level was collected if available but excluded from the survival analyses because of many missing data.

The Fisher exact tests were used for the descriptive statistical analyses on categorical data. Overall survival (OS) and progression free survival (PFS, time from diagnosis to disease progression, relapse or death of any cause) were calculated using Kaplan–Meier method (5) and was compared between two groups by log-rank test. Logistic regression models were used to evaluate the associations between multiple characteristics and complete response (CR). Patient characteristics were also analyzed for their association with PFS and OS using Cox proportional hazard models. In this model, characteristics with P-values <0.10 in the univariate analyses were included in the multivariate analyses, and a backward elimination with a P-cutoff of 0.05 was used. All computations were performed in STATA version 9.0 (StataCorp, College Station, TX, USA).

Results

Patient characteristics

Patient characteristics are summarized in Table 1. There was no significant difference in baseline characteristics between CHOP and RCHOP group. In patients with early-stage non-bulky disease, involved field radiation therapy was performed following three courses of CHOP (n = 37) or RCHOP (n = 38) therapy. Patients younger than 65 with age-adjusted IPI score of 2 or 3 were generally offered an option of upfront autologous stem cell transplantation after induction therapy, and 20 such patients (11 after CHOP and nine after RCHOP) underwent this treatment.

The median value of ALC of entire population was 1.20×10^9/L (range $0.10–4.64 \times 10^9$/L). ALC was significantly higher in IPI low risk (median ALC 1.49×10^9/L), and the values were not significantly different among low-intermediate (median 0.97×10^9/L), high-intermediate (median 0.93×10^9/L) and high-risk (median 0.83×10^9/L) groups (Fig. 1). Low ALC [$<1.2 \times 10^9$/L (median value)] was associated with advanced stage, PS ≥2, elevated LDH, number of extranodal involvement ≥2, B symptoms, elevated β2microglobulin and higher IPI risk group. Using different cutoff value of ALC (0.8, 1.0 and 1.4×10^9/L) revealed essentially the same result (data using the cutoff value of 1.0×10^9/L are shown in Table 1).

Treatment response

Response to initial treatment was evaluable in 210 patients, among whom CR rate was 91.9%. CR rates in patients with low and high ALC after CHOP were 85.0% (34/40) and 97.3% (72/74), respectively (P = 0.021). Those after RCHOP were 87.5% (35/40) and 92.9% (52/56), respectively (P = 0.483). Univariate analysis using logistic regression model for the chance of achieving CR revealed that elevated LDH, PS ≥2, number of extranodal involvement ≥2 and presence of B symptoms were significantly associated with lower chance of achieving CR. Low ALC [$<1.2 \times 10^9$/L (median value)] was not significantly associated with low CR rate {odds ratio of low ALC ($<1.2 \times 10^9$/L) = 2.63 [95% confidence interval (CI) 0.894–7.77], P = 0.079}. Other cutoff values (0.8, 1.0 and 1.4×10^9/L) were also tested in association with CR rate, and the association was significant when cutoff value of 1.0×10^9/L was used [odds ratio of low ALC ($<1.0 \times 10^9$/L) for low CR rate = 3.29 (95% CI 1.17–9.30), P = 0.024]. The cutoff value of 1.0×10^9/L was also found to be optimal in the survival analyses as shown later. Higher IPI risk group was also associated with lower CR rate [RR = 1.68 (1.11–2.55), P = 0.014]. Multivariate analysis revealed that only PS ≥2 [RR = 5.47 (1.87–16.0), P = 0.002] and elevated LDH [RR = 4.66 (1.25–17.3), P = 0.022] were independently associated with lower CR rate.

Overall survival

The median follow-up duration in the entire population, CHOP and RCHOP groups were 47, 67 and 29 months, respectively. Two-year OS rates in CHOP and RCHOP groups were 82.1 ± 3.6% and 87.0 ± 3.7%, respectively. The Kaplan–Meier OS estimate curves were first plotted according to ALC groups (<0.61, 0.61–0.80, 0.81–1.00, 1.01–1.20, 1.21–1.40, 1.41–1.60 and $>1.60 \times 10^9$/L) to find the optimal cutoff value to define low and high ALC groups. This revealed that OS was generally longer in patients with higher ALC and curves

Table 1 Patient characteristics

Parameters	*n* (total 221)	ALC < 1.0×10^9/L	*P*-value	Rituximab	*P*-value
All	221	86		102	
Age (yr)					
≤60	106	37	0.270	47	0.686
>60	115	49		55	
Stage					
1/2	136	35	<0.001	62	0.890
3/4	85	51		40	
PS					
0/1	184	62	0.001	85	1.000
≥2	37	24		17	
LDH					
Normal	119	29	<0.001	51	0.344
High	102	57		51	
Number of extranodal involvement					
0/1	177	58	<0.001	83	0.736
≥2	44	28		19	
B symptoms					
Absent	188	65	0.003	84	0.346
Present	33	21		18	
IPI					
Low	117	26	<0.001	50	0.508
Low-intermediate	37	19		20	
High-intermediate	36	21		19	
High	31	20		13	
Bulky disease (≥10 cm)					
No	202	79	1.000	90	0.150
Yes	19	7		12	
Serum β2microglobulin					
<3.0 mg/dL	98	33	0.036	43	0.683
≥3.0 mg/dL	32	18		16	
NA	91	35		43	
Treatment					
CHOP	119	42	0.269	0	–
RCHOP	102	44		102	
ALC					
<1.0×10^9/L	86	86	–	44	0.269
≥1.0×10^9/L	135	0		58	

PS, Eastern Cooperative Oncology Group Performance Status; LDH, serum lactate dehydrogenase level; B symptoms, presence of at least one of the followings – night sweat, weight loss >10% over 6 months and recurrent fever >38.3°C; IPI, International Prognostic Index; ALC, absolute lymphocyte count; NA, not available.
P-values were calculated by Fisher exact test.

were grossly separated at a cutoff value of 1.0×10^9/L (data not shown). To confirm the optimal cutoff values for determining 'low ALC', we next performed sensitivity analysis, where among candidate cutoff values of 0.8, 0.9, 1.0, 1.1, 1.2, 1.3 and 1.4×10^9/L, the maximal hazard ratio (HR) was produced with the cutoff value of 1.0×10^9/L [HR = 2.89 (95% CI 1.61–5.17)]. Low ALC was thus defined to be $< 1.0 \times 10^9$/L for further survival analyses. The Kaplan–Meier OS estimate curves, calculated according to treatment (CHOP and RCHOP) and ALC (high and low) are shown in Fig. 2A. In CHOP group, 2-yr OS rates in patients with high and low ALC were 90.7 ± 3.6% and 66.5 ± 7.3%, respectively. Those in RCHOP group were 92.1 ± 3.8% and 79.8 ± 7.0%, respectively. By univariate analysis using Cox proportional hazard model, low ALC was associated with shorter OS duration in the entire population [HR = 2.89 (1.61–5.17), $P < 0.001$] or in CHOP group [HR = 3.61 (1.81–7.20), $P < 0.001$] but the difference was not significant in RCHOP group [HR = 1.78 (0.599–5.32), $P = 0.298$].

Multivariate analysis for OS incorporating all the characteristics except IPI risk group revealed that PS ≥2 [HR = 3.34 (1.82–6.15), $P < 0.001$], low ALC [HR = 2.51 (1.38–4.58), $P = 0.003$] were independently associated with shorter OS. In this model, rituximab was forced in the analysis [HR = 0.530 (0.276–1.02), $P = 0.057$]. Furthermore, when IPI risk group (analyzed

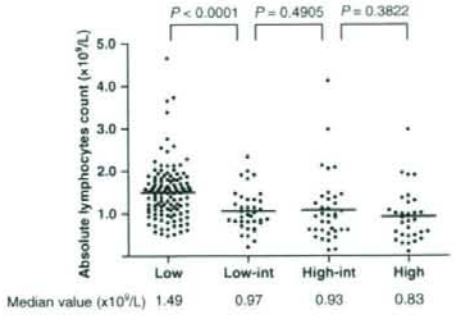

Figure 1 Absolute lymphocyte count according to IPI risk group.) *P*-values were calculated by non-parametric non-paired *t*-test (Man-Whitney test).

as a linear parameter) was incorporated instead of five IPI factors (i.e. age, PS, LDH, stage and number of extranodal involvement were omitted), low ALC was associated with shorter OS [HR = 2.11 (1.12–3.95), $P = 0.019$], along with IPI group [HR 1.50 (1.16–1.92), $P = 0.002$], where rituximab was again forced in the model [HR = 0.531 (0.278–1.02), $P = 0.056$, Table 2]. Removing rituximab from the final model showed the similar result for both analyses. Analyzing IPI risk group as a categorical parameter also showed essentially the same result [HR of low ALC = 2.05 (1.09–3.86), $P = 0.026$, Table 2].

Given that the baseline patient characteristics were similar in CHOP and RCHOP group (Table 1), OS was next compared between CHOP and RCHOP groups, according to ALC group. Use of rituximab was associated with longer OS in low ALC group [HR = 0.42 (0.18–1.00), $P = 0.05$] but not in high ALC group [HR = 0.83 (0.31–2.21), $P = 0.71$]. This suggests that the prognostic significance of ALC became smaller in the era of rituximab, as shown earlier, because the absolute survival benefit from rituximab is larger in low ALC group than in high ALC group (Fig. 2A). To further evaluate the significance of ALC and rituximab use, we next performed subgroup analyses of OS based on IPI risk group (Fig. 2B,C). In this analyses, we defined two IPI risk group [score '0–1' ($n = 117$) and '2–5' ($n = 104$)] because of significantly higher ALC distribution only in '0–1' group (Fig. 1), and limited number of patients in each low-intermediate, high-intermediate and high-risk group. The use of rituximab in patients with IPI '2–5' group with low ALC was associated with longer OS [HR = 0.35 (0.12–0.98), $P = 0.045$], but not in IPI '2–5' with high ALC [HR = 1.02 (0.33–3.13), $P = 0.978$], or in IPI '0–1' with low ALC [HR = 0.83 (0.15–4.44), $P = 0.824$] or in IPI '0–1' with high ALC [HR = 0.42 (0.05–3.67), $P = 0.432$].

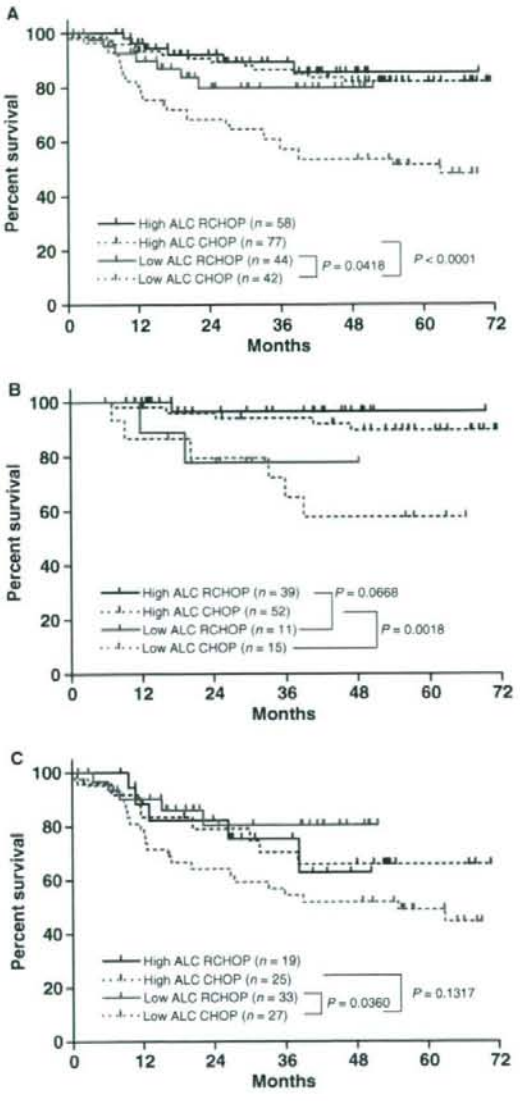

Figure 2 Overall survival according to absolute lymphocyte count and use of rituximab.) (A) All patients; (B) IPI score 0–1; (C) IPI score 2-5. *P*-values were calculated by Log-rank test. *P*-value for any survival comparison was >0.1 if not shown.

Progression free survival

We also performed analyses for PFS. Two-year PFS rates in CHOP group and RCHOP group were 72.8 ± 4.1% and 81.2 ± 4.2%, respectively. In CHOP group, 2-yr PFS rates in high and low ALC groups were 82.8 ± 4.3% and 54.6 ± 7.7%, respectively. In RCHOP group, those were

Table 2 The result of multivariate analyses for OS and PFS when IPI group was analyzed either as a linear parameter or a categorical parameter.

	Hazard ratio	95% CI	*P*-value
For OS			
Low ALC (<1.0 × 10^9/L)	2.11	1.12–3.95	0.019
IPI as a linear parameter	1.50	1.16–1.92	0.002
Rituximab (forced in the model)	0.531	0.278–1.02	0.056
For OS			
Low ALC (<1.0 × 10^9/L)	2.05	1.09–3.86	0.026
IPI			
Low-intermediate vs. low	1.93	0.831–4.49	0.126
High-intermediate vs. low	1.29	0.511–3.27	0.588
High vs. low	3.26	1.19–7.11	0.003
B symptoms	2.37	1.16–4.83	0.018
Rituximab	0.471	0.243–0.915	0.026
For PFS			
Low ALC (<1.0 × 10^9/L)	2.17	1.25–3.76	0.006
IPI as a linear parameter	1.53	1.22–1.91	<0.001
Rituximab	0.452	0.255–0.801	0.007
For PFS			
Low ALC (<1.0 × 10^9/L)	2.22	1.28–3.87	0.005
IPI			
Low-intermediate vs. low	1.52	0.703–3.28	0.287
High-intermediate vs. low	1.72	0.813–3.62	0.156
High vs. low	3.80	1.95–7.44	<0.001
Rituximab	0.457	0.258–0.810	0.007

84.0 ± 5.3% and 77.8 ± 6.6%, respectively. By univariate analysis using Cox proportional hazard model, low ALC was associated with shorter EFS duration in the entire population [HR = 2.91 (1.75–4.86), $P < 0.001$] or in CHOP group [HR = 3.90 (2.12–7.16), $P < 0.001$] but the difference was not significant in RCHOP group [HR = 1.68 (0.647–4.35), $P = 0.287$]. Multivariate analysis for PFS incorporating all characteristics except IPI group revealed that PS ≥2 [HR = 3.40 (1.98–5.83), $P < 0.001$], low ALC [HR = 2.72 (1.61–4.60), $P < 0.001$] and rituximab [HR = 0.433 (0.242–0.772), $P = 0.005$] were independently associated with shorter PFS. When IPI group as a linear parameter was incorporated instead of five IPI factors, low ALC was again associated with shorter PFS [HR = 2.17 (1.25–3.76), $P = 0.006$], along with IPI group [HR 1.53 (1.22–1.91), $P < 0.001$] and rituximab [HR = 0.452 (0.255–0.801), $P = 0.007$, Table 2]. Analyzing IPI risk group as a categorical parameter also showed similar result [HR of low ALC = 2.22 (1.28–3.87), $P = 0.005$, Table 2].

Discussion

ALC is an objective and reproducible test result, which can be obtained by basic laboratory equipment. Our study demonstrated that low ALC is a poor prognostic factor with regards to OS and PFS. Such prognostic value of ALC is in agree with other recently published studies (3, 6, 7). Although the actual mechanisms of this association between low ALC and poor prognosis is unclear, possibilities include: (i) low ALC may be associated with already immunosuppressed condition, suggesting that the host tends to have an inadequate immunological reaction; (ii) low ALC may be a consequence of lympholytic cytokines produced by lymphoma cells, and such lymphoma may already have a resistant character by itself; or (iii) the combination of these two or other.

The prognostic value of ALC was most remarkable in patients treated with CHOP without rituximab. The difference of prognostic impact between CHOP and RCHOP groups is largely because of the improvement of survival by rituximab in patients with low ALC. Particularly in the group of IPI score 2–5, treatment with rituximab significantly improved survival of patients with low ALC, but not significantly that of patients with high ALC. Analogy of this prognostic value of low ALC is that of expression of BCL2, which was a significant poor prognostic indicator before the emergence of rituximab but not in the era of rituximab (8).

Obvious limitation of this comparison is that salvage regimens might or might not have contained rituximab in relapsed patients in CHOP group (although this would not affect OS), and that the patients were not randomized (although characteristics shown in Table 1 were similar in the two groups). Although not using rituximab in addition to CHOP in any patients with DLBCL may not be justifiable given the little toxicity and significant potential benefit (9, 10), it should be noted that the absolute survival benefit is likely larger in patients with low ALC than in those with high ALC, in the era of multiple target therapy agents (currently approved or not) which may lead to expanding costs with significant impact on the economy.

Acknowledgements

We thank Ryoko Yamauchi and Aki Kobayashi for their excellent secretarial support.

Conflict of interest

None.

Authors' contributions

All authors contributed to the patient care and data collection. Y. O. designed the study, analyzed data and wrote the paper. K. Y. analyzed the data and edited the paper. H. K. and Y. Kuwatsuka edited the paper. H. T. and Y. Kagami reviewed the paper. Y. M. supervised the patient care and edited the paper.

References

1. Hasenclever D, Diehl V. A prognostic score for advanced Hodgkin's disease. International Prognostic Factors Project on Advanced Hodgkin's Disease. *N Engl J Med* 1998;**339**:1506–14.
2. Siddiqui M, Ristow K, Markovic SN, *et al.* Absolute lymphocyte count predicts overall survival in follicular lymphomas. *Br J Haematol* 2006;**134**:596–601.
3. Kim DH, Baek JH, Chae YS, Kim YK, Kim HJ, Park YH, Song HS, Chung JS, Hyun MS, Sohn SK. Absolute lymphocyte counts predicts response to chemotherapy and survival in diffuse large B-cell lymphoma. *Leukemia* 2007;**21**:2227–30.
4. The International Non-Hodgkin's Lymphoma Prognostic Factors Project. A predictive model for aggressive non-Hodgkin's lymphoma. *N Engl J Med* 1993;**329**:987–94.
5. Kaplan EL, Meire P. Nonparametric estimation from incomplete observations. *J Am Stat Assoc* 1958;**53**:457–81.
6. Cox MC, Nofroni I, Laverde G, *et al.* Absolute lymphocyte count is a prognostic factor in diffuse large B-cell lymphoma. *Br J Haematol* 2008;**141**:265–8.
7. Talaulikar D, Choudhury A, Shadbolt B, Brown M. Lymphocytopenia as a prognostic marker for diffuse large B cell lymphomas. *Leuk Lymphoma* 2008;**49**:959–64.
8. Mounier N, Briere J, Gisselbrecht C, *et al.* Rituximab plus CHOP (R-CHOP) overcomes bcl-2 – associated resistance to chemotherapy in elderly patients with diffuse large B-cell lymphoma (DLBCL). *Blood* 2003;**101**:4279–84.
9. Coiffier B, Lepage E, Briere J, *et al.* CHOP chemotherapy plus rituximab compared with CHOP alone in elderly patients with diffuse large-B-cell lymphoma. *N Engl J Med* 2002;**346**:235–42.
10. Pfreundschuh M, Trumper L, Osterborg A, *et al.* CHOP-like chemotherapy plus rituximab versus CHOP-like chemotherapy alone in young patients with good-prognosis diffuse large-B-cell lymphoma: a randomised controlled trial by the MabThera International Trial (MInT) Group. *Lancet Oncol* 2006;**7**:379–91.

De novo CD5+ diffuse large B-cell lymphoma: results of a detailed clinicopathological review in 120 patients

Motoko Yamaguchi,[1] Naoya Nakamura,[2] Ritsuro Suzuki,[3] Yoshitoyo Kagami,[4] Masataka Okamoto,[5] Ryo Ichinohasama,[6] Tadashi Yoshino,[7] Junji Suzumiya,[8] Takuhei Murase,[9] Ikuo Miura,[10] Koichi Ohshima,[11] Momoko Nishikori,[12] Jun-ichi Tamaru,[13] Masafumi Taniwaki,[14] Masami Hirano,[5,15] Yasuo Morishima,[4] Ryuzo Ueda,[16] Hiroshi Shiku,[1] and Shigeo Nakamura[1]

[1]Mie University Graduate School of Medicine, Tsu; [2]Tokai University, Isehara; [3]Nagoya University Graduate School of Medicine, Nagoya; [4]Aichi Cancer Center, Nagoya; [5]Fujita Health University School of Medicine, Toyoake; [6]Tohoku University Postgraduate School of Medicine, Sendai; [7]Okayama University Graduate School of Medicine and Dentistry, Okayama; [8]Fukuoka University Chikushi Hospital, Fukuoka; [9]Nishio Municipal Hospital, Nishio; [10]St. Marianna Medical University, Kawasaki; [11]Kurume University School of Medicine, Kurume; [12]Kyoto University, Kyoto; [13]Saitama Medical Center, Kawagoe; [14]Kyoto Prefectural University of Medicine, Kyoto; [15]Meijo University, Nagoya, and [16]Nagoya City University Medical School, Nagoya, Japan

Acknowledgments: we thank the collaborators from the institutions for providing patients' data and specimens. A list of participating institutes is given in the Appendix. This paper was presented in part at the 49th Annual Meeting of the American Society of Hematology, Atlanta, December 2007.

Funding: this work was supported in part by Grants-in-Aid for Cancer Research (15-11, 19-8) from the Ministry of Health, Labour and Welfare, Japan.

Manuscript received January 24, 2008. Revised version arrived on March 26, 2008. Manuscript accepted April 15, 2008.

Correspondence:
Motoko Yamaguchi, M.D., Ph.D., Department of Hematology and Oncology, Mie University Graduate School of Medicine, 2-174 Edobashi, Tsu, Mie 514-8507, Japan.
E-mail: waniwani@clin.medic.mie-u.ac.jp

ABSTRACT

Background
De novo CD5-positive diffuse large B-cell lymphoma (CD5+ DLBCL) is clinicopathologically and genetically distinct from CD5-negative (CD5−) DLBCL and mantle cell lymphoma. The aim of this retrospective study was to clarify the histopathological spectrum and obtain new information on the therapeutic implications of CD5+ DLBCL.

Design and Methods
From 1984 to 2002, 120 patients with CD5+ DLBCL were selected from 13 collaborating institutes. We analyzed the relationship between their morphological features and long-term survival. The current series includes 101 patients described in our previous study.

Results
Four morphological variants were identified: common (monomorphic) (n=91), giant cell-rich (n=13), polymorphic (n=14), and immunoblastic (n=2). Intravascular or sinusoidal infiltration was seen in 38% of the cases. BCL2 protein expression in CD5+ DLBCL was more frequent than in CD5− DLBCL (p=0.0003). Immunohistochemical analysis in 44 consecutive cases of CD5+ DLBCL revealed that 82% of these cases (36/44) were non-germinal center B-cell type DLBCL. The 5-year overall survival rate of the patients with CD5+ DLBCL was 38% after a median observation time of 81 months. Patients with the common variant showed a better prognosis than those with the other three variants (p=0.011), and this was confirmed on multivariate analysis. Overall, 16 patients (13%) developed central nervous system recurrence.

Conclusions
Our study revealed the morphological spectrum of CD5+ DLBCL, found that the incidence of central nervous system recurrence in this form of lymphoma in high, confirmed that CD5+ DLBCL frequently expresses BCL2 protein and showed that it is mainly included in the non-germinal center B-cell type of DLBCL.

Key words: diffuse large B-cell lymphoma, CD5, histopathology, BCL2, central nervous system.

Citation: Yamaguchi M, Nakamura N, Suzuki R, Kagami Y, Okamoto M, Ichinohasama R, Yoshino T, Suzumiya J, Murase T, Miura I, Ohshima K, Nishikori M, Tamaru J, Taniwaki M, Hirano M, Morishima Y, Ueda R, Shiku H and Nakamura S. De novo CD5+ diffuse large B-cell lymphoma: results of a detailed clinicopathological review in 120 patients. Haematologica 2008; 93:1195-1202. doi: 10.3324/haematol.12810

Introduction

Diffuse large B-cell lymphoma (DLBCL) constitutes the largest category of aggressive lymphomas, and is considered to have heterogeneous biological properties.[1,2] The phenomenon of CD5 expression in DLBCL evolving *de novo*, and not as a result of the transformation of chronic lymphocytic leukemia and mantle cell lymphoma, was first described by Matolcsy *et al.* in 1995.[3] Since then, accumulating clinicopathological evidence has gradually clarified that *de novo* CD5-positive ($CD5^+$) DLBCL constitutes a unique subgroup of DLBCL.[4-13] *De novo* $CD5^+$ DLBCL is associated with onset in old age, female predominance, advanced stage at diagnosis, the presence of B symptoms, high levels of lactate dehydrogenase, and the frequent involvement of extranodal sites. The genetic analysis of this lymphoma has suggested that it may originate from somatically mutated $CD5^+$ progenitor B cells.[5,6,8,13] Moreover, an analysis using cDNA microarray and comparative genomic hybridization technology demonstrated that *de novo* $CD5^+$ DLBCL is distinct from $CD5^-$ DLBCL and mantle cell lymphoma.[12,14-17] Cytogenetic analysis identified a subgroup of patients with *de novo* $CD5^+$ DLBCL with chromosomal abnormalities in 8p21 or 11q13 who have a poor prognosis.[18]

We reported that *de novo* $CD5^+$ DLBCL tumors usually show a centroblastic morphology, and 19% show an intravascular or sinusoidal growth pattern.[11] However, CD5 is expressed in some cases of intravascular large B-cell lymphoma[19-22] and T-cell-rich B-cell lymphoma,[23] and cases of $CD5^+$ follicular lymphoma[24,25] and $CD5^+$ Burkitt's lymphoma[26] have been reported. The relationship between these tumors and *de novo* $CD5^+$ DLBCL remains to be clarified. We reported that *de novo* $CD5^+$ DLBCL shows an aggressive clinical course, with a 5-year overall survival rate of 34%.[11] However, the median observation period in our previous study was 33 months; the results should, therefore, be confirmed by long-term survival analysis.

To clarify the histopathological spectrum of $CD5^+$ DLBCL and obtain new information on the therapeutic implications, we performed a detailed clinicopathological review and long-term follow-up analysis in a larger number of patients with *de novo* $CD5^+$ DLBCL.

Design and Methods

Patients

We selected 120 patients with *de novo* $CD5^+$ DLBCL from 13 collaborating institutes. All patients were diagnosed between 1984 and 2002 as having DLBCL according to the WHO classification,[2] and they had no past history of any other lymphoproliferative disorders. All specimens for histological and immunophenotypic studies were obtained at the initial presentation of the patients, and were examined for CD5 antigen expression by means of flow cytometry and/or immunohistochemistry. All patients were immunohistochemically confirmed to be cyclin D1-negative. The current series includes 101 of 109 *de novo* $CD5^+$ DLBCL cases described in our previous study.[11] Seven patients who fulfilled the diagnostic criteria for intravascular large B-cell lymphoma[2] and one patient with follicular colonization were excluded. The study was approved by the Ethics Committee of Mie University Graduate School of Medicine, and complied with the Helsinki Declaration.

Clinical information was obtained from the hospital records or supplied by the physicians at the collaborating centers.

Morphological evaluation

Tissue was fixed in 10% formalin and embedded in paraffin. Sections (5 μm thick) were stained with hematoxylin and eosin. We examined all the 120 initial diagnostic specimens of the *de novo* $CD5^+$ DLBCL cases, consisting of 85 lymphatic tissues such as lymph node, Waldeyer's ring, and spleen and 35 extranodal tissues with lymphomatous involvement. All cases were blindly reviewed twice by three of the authors (*MY, NN, and SN*). If discrepancies occurred, we discussed the cases while using a multiheaded microscope to reach a consensus.

Immunophenotypic study

Immunohistochemical and flow-cytometric analyses were performed as described previously.[27,28] The monoclonal antibodies used were Leu4 (CD3), Leu1 (CD5), and CALLA (CD10) (Becton Dickinson, Mountain View, CA, USA); J5 (CD10) and B1 (CD20) (Coulter, Hialeah, FL, USA); H107 (CD23) (Nichirei, Tokyo, Japan); MHM6 (CD23), BerH2 (CD30), UCHL1 (CD45RO), HM57 (CD79a), anti-immunoglobulin (Ig)G, anti-IgA, anti-IgM, anti-IgD, anti-kappa, and anti-lambda (DAKO, Carpentaria, CA, USA); 4C7 (CD5) and NCL-CD10 (CD10) (Novocastra, Newcastle, UK), and cyclin D1 (IBL, Gunma, Japan). More than 20% positivity of the tumor cells was considered to indicate positivity for the purposes of this study. Based on preliminary data that the incidence of CD5 positivity in DLBCL examined with paraffin material is approximately half of that examined using frozen sections, and that it can be increased using more sensitive immunohistochemical methods (*Yamaguchi M et al., presented at the Annual Meeting of the Japanese Society of Lymphoreticular Tissue Research, 2000*), CD5 expression was examined primarily by flow cytometry and/or immunohistochemistry in the frozen sections from 104 cases of *de novo* $CD5^+$ DLBCL. In the remaining 16 cases, CD5 expression was examined immunohistochemically using paraffin-embedded sections. In fact, 75% or more of the neoplastic cells were confirmed to be positive for CD5 in the cases examined using paraffin-embedded material alone.

BCL2 protein expression was examined by means of immunohistochemistry using paraffin sections and a monoclonal antibody (BCL2, DAKO). Paraffin-embedded material for this study was available in 96 out of 120 cases. Staining for BCL2 was performed at the Aichi Cancer Center, and the data were compared with those for 150 cases of $CD5^-$ DLBCL, which were sequentially diagnosed at the Aichi Cancer Center during the same period as the *de novo* $CD5^+$ DLBCL cases. The reaction

for BCL2 protein was classified as positive if more than 50% of lymphoma cells were stained.[29]

We also classified *de novo* CD5⁺ DLBCL into two subgroups, i.e., germinal center B-cell and non-germinal center B-cell types.[30] From the file of histological consultation for diagnosis at the Aichi Cancer Center in the period from 2000 to 2004, 44 cases of *de novo* CD5⁺ DLBCL were selected for this analysis. Staining for CD10, BCL6 (NCL-BCL6, Novocastra), and MUM1 (MUM1p, DAKO) was performed on paraffin sections.[30] Cases were considered positive if 30% or more of the neoplastic cells were stained with an antibody. Subsequently, each case was classified into germinal center or non-germinal center B-cell types according to the criteria of Hans *et al.*[30]

Statistical analysis

Correlations between the two groups were examined with the χ^2 test and Fisher's exact test. Patients' survival data were analyzed with the Kaplan-Meier method and were compared by means of the log-rank test. Univariate and multivariate analyses were performed with the Cox proportional hazard regression model, and data were analyzed with STATA software (version 9.0, STATA Corp., College Station, TX, USA).

Results

Histopathological review and characterization of morphological variants

At a low magnification, total or partial effacement of the nodal architecture with a diffuse (118 patients, 98%) or vaguely nodular pattern (2 patients, 2%) of tumor cell proliferation was observed. In ten patients (8%), these tumor cells were distributed throughout the interfollicular area, while the follicles which had retained their mantle cuffs were spared.

In the current study, particular attention was paid to the presence or absence of intravascular and/or sinusoidal patterns. Although the extent of such patterns varied in each case, they were seen in 45 cases examined (38%). In the specimens of lymph node obtained from 31 patients, tumor cells infiltrated diffusely and focal intrasinusoidal infiltration was observed simultaneously. In the specimens of bone marrow from seven patients, spleen from two patients, and Waldeyer's ring from one patient, lymphoma cells were observed mainly in the sinusoids. In the other patients, a specimen was taken from the tumor in the nasal cavity, stomach, breast, and testis. In those specimens, lymphoma cells infiltrated diffusely, and focal intravascular infiltration was also observed. There was no significant difference in the incidence of intravascular and/or sinusoidal patterns between lymphatic (34/85, 40%) and extranodal (11/35, 31%) specimens.

The size of tumor cells was medium-to-large in 19 cases, mixed medium and large in 14 cases, and large in 87 cases. The tumor cells generally showed a scant or moderate rim of pale baso- or amphophilic cytoplasm. Of note, bi-nucleated tumor cells with a *snowman-like* morphology were frequently observed in our series (101 out of 120 cases, 85%) (Figures 1A and 2B). Apoptotic cells were observed in 21% of the cases.

We classified *de novo* CD5⁺ DLBCL according to cytomorphological features (Figure 1). In 91 (76%) of 120 patients, monomorphic proliferation of typical centroblasts was observed, although a few scattered giant cells were seen in nine patients. We regarded these features as the prototype of *de novo* CD5⁺ DLBCL and referred to it as the common variant. In 13 (11%) out of the remaining patients, there was an increase in very large cells with giant or multiple nuclei, varying from 10 to 30% in area and intermixed with centroblasts and immunoblasts. We referred to this as the giant cell-rich variant. This could correspond to the anaplastic variant of DLBCL according to the WHO classification.[2] While the giant cell-rich variant was thus shown to have a polymorphous composition, monomorphous areas with relatively small cells were also usually identified, suggesting that there is a histological continuum between the common and giant cell-rich variants. CD30 was positive in 23% of the cases (3/13). In 14 patients (12%), tumor cells showed irregularly shaped nuclei,

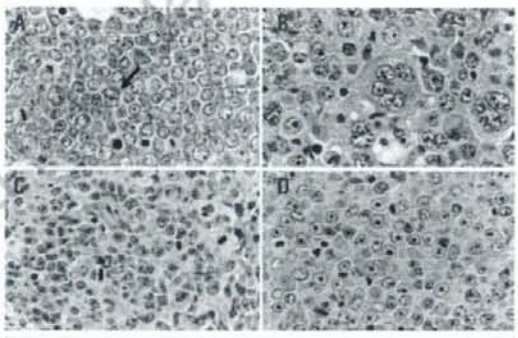

Figure 1. Cytomorphologic features of four variants of *de novo* CD5⁺ DLBCL. The cells, varying from medium to large in size, are uniform, with a pale basophilic or amphophilic cytoplasm. (A) Common variant, which can be described as the monomorphic or centroblastic variant. *Snowman-like*, bi-nucleated cells were seen (arrow). (B) Giant cell-rich variant. (C) Polymorphic variant, characterized by polymorphous proliferation with medium and large-sized cells. The immunoblastic variant (D) was rare in our case series.

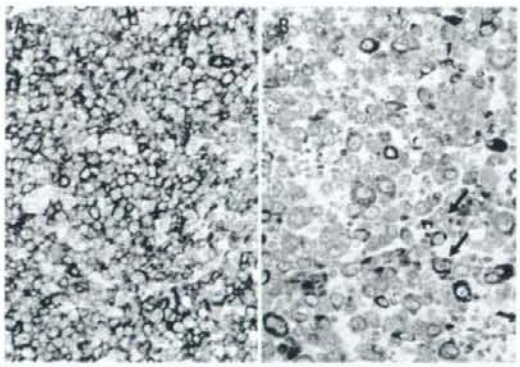

Figure 2. Immunohistochemical features of *de novo* CD5⁺ DLBCL. Lymphoma cells are positive for CD5 (A) and BCL2 (B). *Snowman-like*, bi-nucleated cells can be seen (arrow).